JOURNAL OF MATERIALS SCIENCE 10 (1975) 1938–1942

On the relative fracture surface energies of the major and minor rhombohedra in low-quartz

J. W. HEAVENS, K. H. G. ASHBEE
H. H. Wills Physics Laboratory, University of Bristol, Bristol, UK

The habits of both natural and synthetic crystals of low-quartz reveal that, under conditions of hydrothermal growth, the major rhombohedron $r\{1\,0\,\bar{1}\,1\}$ is more developed than the minor rhombohedron $z\{0\,1\,\bar{1}\,1\}$. The present work demonstrates that this preference of r over z is reversed during fracture. It is also shown that neither the Hartman and Perdok [1] method nor that of Herring [2] can predict any difference in surface energy for r and z but that, by reducing the problem to the fracture or growth of a single SiO_4 tetrahedron, it is possible to account for both observations.

1. Introduction

A basic understanding at the atomic level of fracture in silica and silicates is of fundamental importance to the interpretation and exploitation of both the Rebinder effect and the colloid and surface chemistry of these materials. Continuum theories, although very successful at providing parameters capable of measuring fracture toughness, do not permit discussion of the nature of chemical bonds exposed during fracture.

The investigation of anisotropy of fracture surface energy by uniaxial tensile tests is subject to complications arising from sample differences. To avoid this problem, the present experiments have been limited to studies of Hertzian fracture in basal slabs cut from one large natural crystal of low-quartz. The Hertzian stress field is strongly inhomogeneous and offers the possibility of a wide sampling of fracture surface orientations in one and the same specimen.

2. Experimental

Natural crystals supplied by Gooch and Housego Ltd, of Ilminster, Somerset, were oriented by Laue X-ray back-reflection and sliced with a diamond saw into 10 mm thick slabs perpendicular to the c-axis. The surfaces to be indented were mechanically polished, first with carborundum powders of successively decreasing grain size and finally with a "Selvytt" cloth impregnated with "Silvo". Tests were performed using hardened steel balls of diameters 2, 4, 6 and 8 mm, which were pushed into the slabs by the cross-head of a mechanical testing machine.

3. Description of the Hertzian fracture surface

r and z are both inclined by 52° to the basal plane. However, indentation of the basal plane is mainly accommodated by fracture on z. The ring crack on the surface is very nearly circular (Fig. 1a), indicating that the elastic anisotropy of low-quartz is not so large that it produces a marked departure from the isotropic Hertzian stress field. Well beneath the indented surface, the fracture surface lies between the circular cone of the isotropic case, the shape of which is determined solely by the elastic field, and the triangular pyramid defined by z.

The elastic field caused by pressing a spherical indenter against the flat surface of a block of isotropic material is illustrated by the trajectories in the vertical section through the axis of symmetry shown in Fig. 2. Near the surface the principal stresses are a tensile radial stress σ_1, a hoop stress σ_2 (not shown in the figure) which is tensile except immediately beneath the indenter where it is compressive, and a compressive axial stress σ_3. Further below the surface, the directions of σ_1 and σ_3

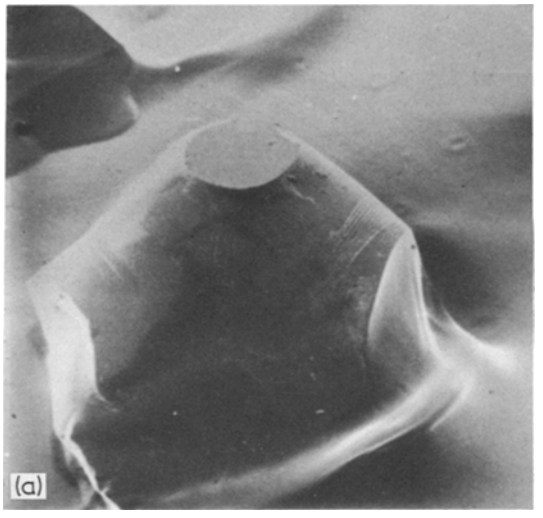

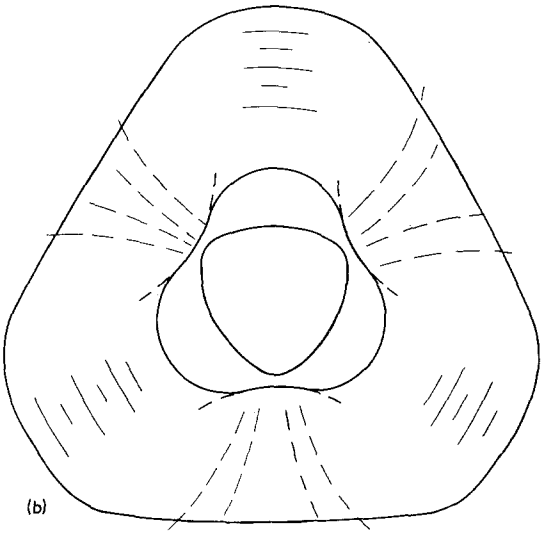

Figure 1 (a) Scanning electron micrograph of a complete cone extracted from a basal slab indented by a 3 mm diameter ball. (b) Sketch of the same fracture surface viewed along c, the symmetry axis. Continuous lines represent horizontal sections of the fracture surface, broken lines indicate the orientations of fracture surface markings. The asymmetry of the innermost continuous line is exaggerated.

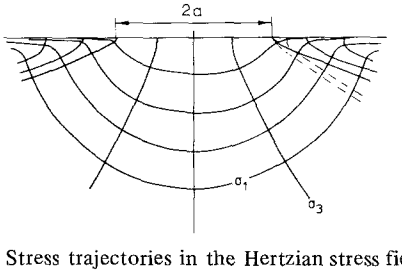

Figure 2 Stress trajectories in the Hertzian stress field. $2a$ is the diameter of the circle of contact. Continuous lines [3], broken lines [4].

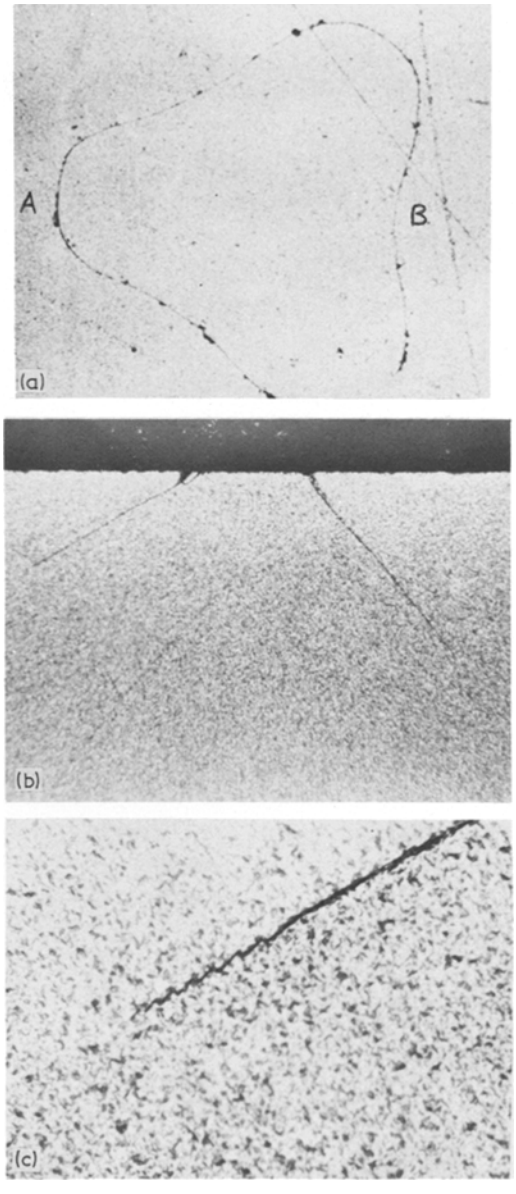

Figure 3 (a) Horizontal section $\frac{1}{3}$ mm below surface of an indented basal slab of low-quartz. (b) Vertical section through AB of (a). (c) Detail of the crack trace on the left hand side of (b).

change as shown. In general, $\sigma_1 > \sigma_2 > \sigma_3$ and the σ_3 stress trajectories leading from near the circle of contact resemble the shape of the fully developed cone crack, i.e. the crack is everywhere approximately normal to σ_1, the largest tensile stress in the elastic field present before fracture. In practice, the identity is not exact. For example, the semi-apex angle of the cone crack in plate glass having a Poisson's ratio of $\nu = 0.22$ is 68° which is a better match with the σ_3 trajectories for $\nu = 0.33$.

At large depths, those parts of the fracture surface corresponding to the rounded edges of the triangular pyramid, see Fig. 3a, exhibit a preference for cleavage on rational planes. Fig. 3b and c show a vertical section through a pyramidal face and clearly reveal alternate fractures on r and z. If the semi-apex angle of $57\frac{1}{2}^\circ$ for the rounded corners puts the crack near the sharp change in direction of σ_1, shown for the isotropic case in Fig. 2, the oscillations between r and z are readily accounted for.

Detailed examination of the fracture surface shown in Fig. 1a reveals two further features worthy of note. Firstly, there is slight asymmetry at the indented surface and this asymmetry is opposite to that below the surface. This is illustrated in Fig. 1b by three continuous lines representing three sections of the fracture surface seen in plan view. Secondly, the crack edge appears to start out with a slight concavity, emphasized in Fig. 1b by projections on the second of the three continuous lines. Concavity of a crack edge is interesting because it would concentrate any perturbations such as hackle markings. That this concavity soon gives way to convexity is evident from the divergence of the hackle markings seen greater depths. It could be that, to begin with, the geometry of the cone fracture surface is determined by the elastic field but that, as soon as the crack edge becomes tangential to z, it dives along the lower surface energy path represented by z.

4. Discussion

The preferred fracture of z over r poses a stringent test of models for calculating surface energies not least because it is opposite to the relative habits of the two rhombohedra obtained during growth from aqueous solution.

Fig. 4 shows an isometric projection of an SiO_4 tetrahedron model of the hexagonal high-quartz structure. In low-quartz the tetrahedra are slightly rotated such that one set of two-fold axes is destroyed. r and z are both perpendicular to the projection, r being parallel to $\mathbf{a}+\mathbf{c}$ and z being parallel to $\mathbf{a}-\mathbf{c}$. Neither the Hartman and Perdok [1] method nor that of Herring [2] can reveal any difference in surface energy between the two planes. Hartman and Perdok identify low energy planes as those which contain periodic bond chain vectors, such as those defined by Si–Si bonds, and these are all parallel to $\mathbf{a}$, $\mathbf{c}$, $\mathbf{a}+\mathbf{c}$ or $\mathbf{a}-\mathbf{c}$. r and z each contain three such vectors. Herring uses a model based on pair-wise interaction energies and assumes that mathematical planes threaded by low densities of nearest neighbour bonds have lowest free energy. Quartz is non-centrosymmetric and the density of bonds intersecting r or z can be varied by translating the mathematical plane along the direction of its pole. This fact complicates application of the Herring treatment. A further, more fundamental problem with the Herring method, pointed out by Frank, is its inability to predict Hauy's law for quartz or, indeed, for any non-centrosymmetric crystal.

Consider the following alternative interpretation of fracture in low-quartz. Ahead of the crack, a half space that supports the stress which is growing the crack can be envisaged. Each element along the crack edge is characterized by a distribution within this half space of silicon atoms, each still bonded to all its nearest neighbours. Since there are three molecules to the unit cell, the

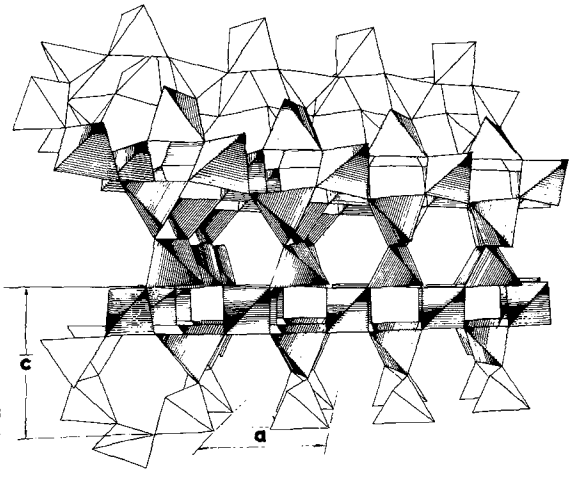

Figure 4 SiO_4 tetrahedron model of quartz. Oxygen atoms are located at the corners and a silicon atom at the body centre of each tetrahedron.

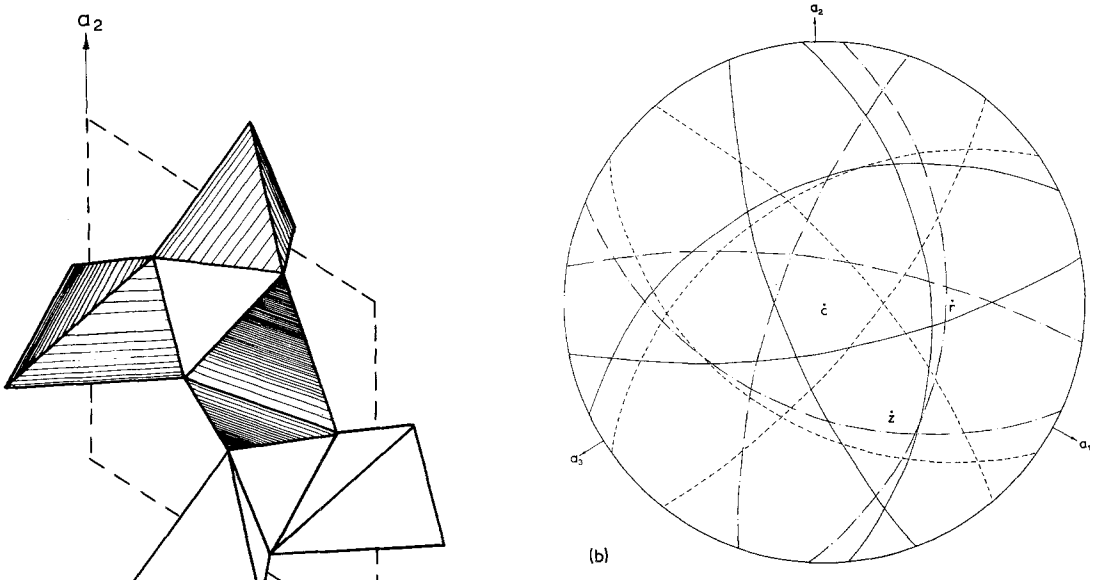

Figure 5 (a) 0 0 0 1 projection of low-quartz showing the three different orientations of SiO_4 tetrahedra. The broken lines define the unit cell. (b) Stereographic projection of the same. The three sets of four great circles are traces to planes defining the faces of the three differently oriented tetrahedra per unit cell. Notice that z is almost normal to one face and, therefore, almost parallel to one triad, belonging to each of two tetrahedra. r is nearly parallel to an edge and, therefore, nearly parallel to a $\bar{4}$-axis, for each of two different tetrahedra.

tetrahedral arrangement of the four oxygen atoms around each silicon atom may be in any of three different spatial kinds, refer to Fig. 5a. If the crack is running more or less perpendicular to a triad of a tetrahedron, it has a choice of paths; either one or three silicon–oxygen bonds is broken. If it is running more or less perpendicular to the $\bar{4}$-axis, two silicon–oxygen bonds are broken. The easiest path is presumably the one which scissions only one silicon–oxygen bond and the fact revealed in Fig. 5a and b that z is very nearly parallel to a triad belonging to each of two of the three differently oriented tetrahedra whereas r is very nearly parallel to a $\bar{4}$-axis for each of two of the three tetrahedra explains why z has the lower fracture surface energy.

The two kinds of atomic configurations exposed by the two possible fracture paths perpendicular to a triad are the respective origins of siloxane and silonal groups produced during the wet fracture of quartz. The concentration of siloxane groups detected by ion exchange reactions [5] heavily outweighs the concentration of silonal groups and confirms that the path which breaks only one silicon–oxygen bond is preferred. During crystal growth, the high and low energy variants perpendicular to a triad must alternately exist and the mean of the associated energies, weighted by a factor of $\frac{2}{3}$ in favour of the lower value because the changeover occurs at the centre of the tetrahedron, is large enough to reverse the relative surface energies of r and z.

If the Herring [2] theorems were applicable, the data shown in Fig. 5b could be used to deduce the shape of the γ^{-1}-polyhedron for Si–O bonds. Over a solid angle about any bond direction in a centro-symmetric crystal there is a range of orientations of planes for which the number of such bonds intersected is constant. For this reason, a polar diagram of surface free energy γ is similar in appearance to the surface of a raspberry; it is constructed from spheres drawn through the origin. Frank [6] has pointed out that a geometrically simpler representation of anisotropy in surface energy is the γ^{-1}-polyhedron, obtained by inverting these spheres through the origin when they become planes. Each great circle in Fig. 5b is the projection of the intersection, with the sphere of projection, of the plane containing the centre and an edge of the Si–O γ^{-1}-polyhedron. Intersections between great circles denote the directions of vectors from the polyhedron centre to its corners.

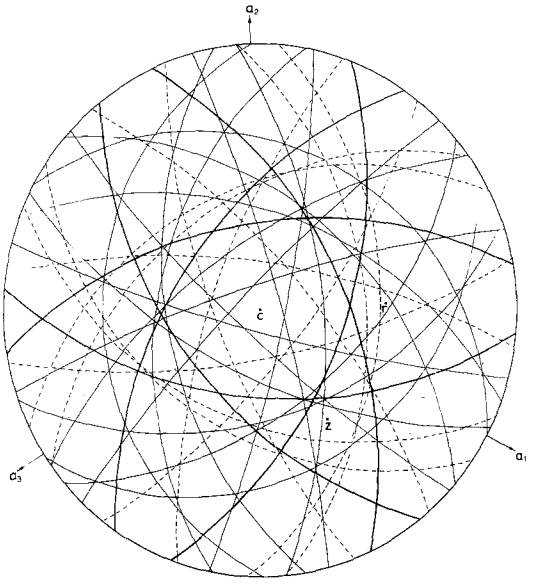

Figure 6 Stereographic projection of low-quartz. Heavy circles denote zones of poles normal to Si–Si bonds, light circles denote zones of poles normal to O–O bonds, and broken circles denote zones of poles normal to Si–O bonds.

The shapes of the γ^{-1} polyhedra for Si–Si, O–O and for Si–O bonds respectively are summarized by the stereographic projection shown in Fig. 6. To use this information it is necessary to make simplifying assumptions. For example, in the wet fracture of quartz it may be that Si–Si bonds are of over-riding importance; by donating a proton to one tetrahedron and a hydroxyl group to its neighbour, each pair of tetrahedra may be separated without introducing any O–O or Si–O contributions to the overall fracture surface energy. Hence, it might be assumed that the Si–Si γ^{-1}-polyhedron is applicable. Referring to Fig. 6, the sectors which contain **a** or **c** each represent γ-invariant orientations in a fracture model based on the density of Si–Si nearest neighbours alone. As a consequence of the non-centrosymmetric crystal structure of low-quartz, all other sectors are γ-variant; the number of Si–Si bonds intersected by any mathematical plane lying within one of these sectors can be varied simply by moving the plane in the direction of its pole. Herring's [2] treatment gives an average value for γ and, since the great circle denoting the boundary between a γ-invariant and a γ-variant sector represents equal γ for both sectors, there must be paths in the γ-variant sector for which γ is higher than for fracture corresponding to the γ-invariant sector. Hence it may be acceptable to assume that the γ^{-1}-polyhedron for the wet fracture of low-quartz is simply the hexagonal prism obtained by extending the γ-invariant sectors, i.e. the hexagonal prism with base perpendicular to **c** and walls perpendicular to **a**.

Acknowledgement

The authors gratefully acknowledge numerous stimulating discussions with Professor F. C. Frank, F.R.S.

References

1. P. HARTMAN and W. G. PERDOK, *Acta. Cryst.* 8 (1955) 49.
2. C. HERRING, *Phys. Rev.* **82** (1951) 87.
3. B. R. LAWN, *J. Appl. Phys.* **39** (1968) 4828.
4. J. W. HEAVENS, University of Bristol Ph.D. Thesis (1972).
5. H. P. BOEHM, *Angew Chemie, Int. Ed.* **5** (1966) 533; *Adv. Catalysts* **16** (1966) 179.
6. F. C. FRANK, ASM Seminar on "Metal Surfaces, Structure, Energetics and Kinetics", (American Society for Metals, Cleveland, Ohio, 1963) Ch. 1.

Received 26 March and accepted 28 April 1975.